



RESEARCH ARTICLE

Wearable Laser Doppler Flowmetry and Fluorescence Spectroscopy Devices: Instrumentation and Methodology of Application in Clinical and Space Research

Elena V. Zharkikh¹  | Yulia I. Loktionova¹  | Vyacheslav S. Yanushin¹  | Kirill S. Kireev^{1,2}  | Victor V. Sidorov³  | Andrey V. Dunaev¹ 

¹Research and Development Center of Biomedical Photonics, Orel State University Named After I.S. Turgenev, Orel, Russia | ²Yu.A. Gagarin Research and Test Cosmonaut Training Center, Zvyozdny gorodok, Russia | ³“SPE LAZMA” Ltd., Moscow, Russia

Correspondence: Elena V. Zharkikh (ev.zharkikh@gmail.com)

Received: 9 October 2025 | **Revised:** 5 December 2025 | **Accepted:** 15 December 2025

Keywords: fluorescence spectroscopy | laser doppler flowmetry | microcirculatory-tissue system | space medicine | wearable device

ABSTRACT

The work aims to study the latest technical developments in instrumental support of laser Doppler flowmetry (LDF) and fluorescence spectroscopy (FS) methods and to evaluate the possibilities of using wearable LDF and FS devices in clinical practice and space medicine. The paper demonstrates the principle of the implementation of wearable LDF and FS devices, the possibilities of forming distributed analyser systems for simultaneous registration of parameters in several areas of interest, and demonstrates examples of registered signals. Prospects and directions of device application in clinical practice are estimated. For the first time, research was conducted to demonstrate the possibility of using wearable LDF and FS devices to record physiological parameters of astronauts in real time during pre-flight training with exposure to overloads, hypoxia and hypobaria, orthostatic and vestibular effects.

1 | Introduction

Monitoring of human physiological parameters is an important aspect of research involving exposure to extreme environmental factors, including studies for space medicine. Prolonged exposure of astronauts to spaceflight factors affects their health, leading to various adverse effects, including decreased bone density and muscle atrophy [1]. Space flight factors that have an unfavourable impact on astronauts' health include microgravity, increased radiation exposure, overloads and long periods of isolation. It is especially important to monitor the state of the cardiovascular system (CVS) of the cosmonaut's organism, as the impact of microgravity leads to redistribution of intercellular fluid in the thorax-head position, resulting in CVS deconditioning, decreased myocardial mass and impaired blood pressure regulation processes [2, 3].

A large amount of valuable diagnostic information on the functioning of the cardiovascular system can be provided by studying the parameters of the microcirculatory-tissue system (MTS), which is the end link of the cardiovascular system and includes not only the capillary network but also microlymph vessels, nerve endings and biotissue cells. MTS is the first to enter the cascade of adaptive reactions under the influence of external factors and pathological changes. It is known that microcirculatory disorders precede the development of such diseases as arterial hypertension, ischaemic heart disease, diabetes mellitus (DM), etc. [4, 5]. Nowadays, various non-invasive methods, mostly based on the application of photonics technologies, have gained popularity for assessing the state of microcirculatory-tissue systems. One of such methods is the laser Doppler flowmetry (LDF). The method is based on probing tissues with laser radiation and analysing the light

scattered by tissues. The light scattered from moving erythrocytes in the biological tissue undergoes a Doppler frequency shift, while the frequency of light scattered from stationary objects remains unchanged [6]. LDF allows to assess not only the general local perfusion of biological tissues but also provides information on the functioning of mechanisms regulating the microcirculatory bed, including endothelial function, neural innervation and intrinsic myogenic regulation of vascular tone [7–9].

LDF, first developed in 1977 [10] has already found wide application in studies aimed at developing methods for early diagnosis of conditions associated with the development of peripheral circulatory disorders. LDF has proven itself in the diagnosis of complications of DM [11–13], arterial hypertension [14], rheumatic diseases [15] and many other pathological conditions. The increasing popularity of wearable medical devices in recent years is also driving interest in the development of wearable LDF devices. There have been several earlier attempts to develop a portable LDF device that does not require the use of optical fibres [16, 17]. Since 2018, production of wearable devices implementing LDF has been established by the Russian company ‘LAZMA’ Ltd. [18, 19], ‘LAZMA PF’ laser blood microcirculation analyser. Currently, ‘LAZMA PF’ devices are available with two diagnostic channels—LDF and fluorescence spectroscopy (FS).

FS is another method that significantly expands the diagnostic capabilities of LDF when used simultaneously. Based on the registration of autofluorescence signal of endogenous fluorophores in biotissue, FS allows estimating the content of such important coenzymes as NADH and FAD—participants of the Krebs cycle. FS has found wide application in various fields of medicine due to its non-invasiveness, non-destructiveness and high sensitivity in detecting biochemical interactions on a molecular scale [20]. A multimodal approach based on the simultaneous application of the two mentioned diagnostic technologies practically in one diagnostic volume allows obtaining complex information about the state of blood supply of biological tissues and their oxidative metabolism and presents great prospects for the development of new diagnostic technologies [21]. However, despite the many advantages and non-invasive diagnostic possibilities offered by the FS method, in non-invasive skin fluorescence studies, the recorded signal is influenced by a large number of factors, including the collagen content, which has its own fluorescence, the absorption of optical radiation by skin melanin, as well as the tissues’ blood filling, which may change, for example, as a result of the pathological processes development or local pressure applied to the biotissue [22]. To eliminate the influence of these factors on the resulting signal, various approaches are used, including normalisation of the recorded fluorescence signal by the intensity of back-reflected radiation at the excitation wavelength.

In recent years, the need to develop new wearable diagnostic devices for space medicine has become more and more evident. The limited space of the International Space Station (ISS) places increased demands on the size of scientific and diagnostic devices delivered to the ISS. In this regard, earlier stationary versions of multimodal devices implementing LDF and FS were not feasible for use in the ISS environment. The emergence of new

portable variations of devices implementing LDF and FS opens new opportunities in the study of microcirculation and oxidative metabolism in space medicine. The aim of the present work was to study the latest technical developments in instrumental support of laser Doppler flowmetry and fluorescence spectroscopy methods in a wearable version and to evaluate the possibilities of application of wearable LDF and FS devices in clinical practice and space medicine.

2 | Technical Implementation of A Wearable Device

Conceptual design of specific optical diagnostic systems for biomedical applications, and even more so in a wearable version, requires careful selection of various technical parameters, including probing wavelength, coherence, polarisation and intensity profile of the incident light, photodetector sensitivity, size as well as geometry and mutual position of the source and detector (measurement base), etc. [23]. In this regard, at the stage of substantiation of medical and technical requirements to the developed device for its further application in clinical and space medicine, a number of calculations, including Monte Carlo simulation of optical radiation propagation in biological tissues, were performed [24]. The physical appearance of wearable devices implementing LDF and FS channels, as well as their operation principle are presented in Figure 1.

Portable multimodal optical spectroscopy device contains 2 sources of optical radiation: laser with a wavelength of 850 nm as a source of radiation of LDF channel and LED with a wavelength of 365 nm as a source of radiation of FS channel. The radiation sources are controlled by drivers. The radiation enters the biological object, where it is partially scattered and absorbed. The backscattered part of radiation from irradiation of biological tissue with light of 850 nm wavelength, when it passes through optical filters, is registered by photodetectors connected with the differential block of Doppler signal processing. The part of optical radiation reflected back from biological structures when probing with 365 nm light and the signal of fluorescence of biological tissues are received and registered by photodetectors equipped with narrow-band optical filters, providing maximum sensitivity at the wavelengths of fluorescence excitation radiation (365 nm) and fluorescence (460 nm), after which the signals arrive at the inputs X and Y of the voltage divider, forming the ratio $Z = Y/X$ at the output of the divider.

The data from the output of the voltage divider, as well as from the Doppler signal processing unit, are delivered to the data acquisition and transmission device, from where they are transmitted via wireless data protocol (Bluetooth/Wi-Fi) to the data processing unit implemented on a personal computer. The device is also equipped with additional channels for registration of skin temperature in the measurement area and the subject’s movements in the process of data registration to eliminate the potential influence of these factors on the measurement results. The device operation is controlled from a personal computer via specialised software.

A vertical-cavity surface-emitting laser (VCSEL) with a centre wavelength of 850 nm and an output power not exceeding

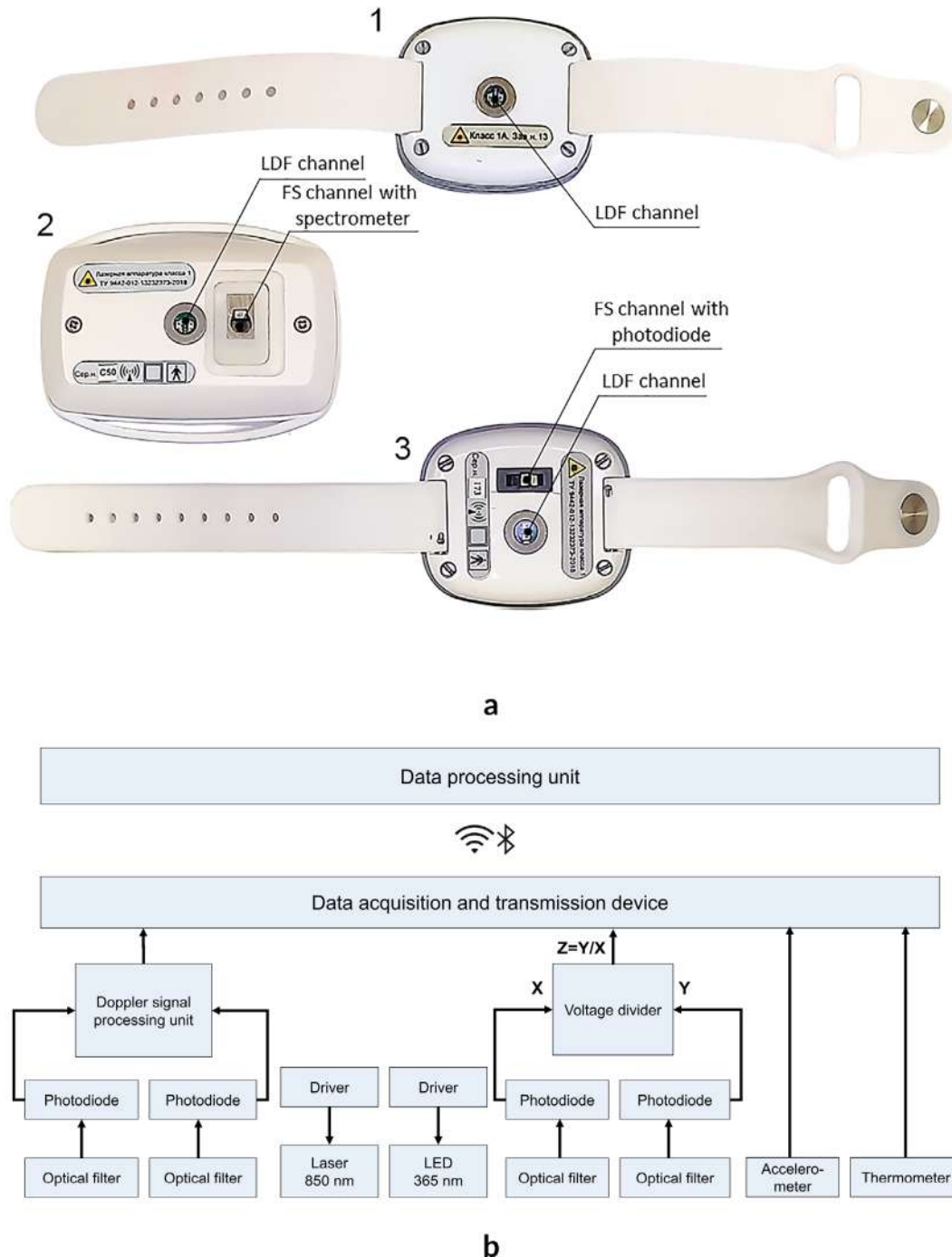


FIGURE 1 | (A) Three versions of wearable devices: 1—devices implementing only the LDF channel, 2—devices implementing LDF channel and FS channel with the use of a miniature spectrometer, 3—devices implementing LDF channel and FS channel with the use of narrow spectral filters and photodetectors; (B) Functional circuit diagram explaining the operating principle of the device.

0.8 mW is used as a radiation source in the LDF channel [25]. For the first time the prospects of VCSEL lasers application for the development of portable LDF devices were evaluated in the work of 2006 [17], where the authors demonstrated the advantages of implementing LDF devices in a fibreless design, which allows to significantly reduce the influence of motion artefacts on the recorded perfusion signal and improve the signal-to-noise ratio. In the demonstrated device, optical radiation from both diagnostic channels is delivered to the biological tissue without using optical fibre directly through a window in the back panel of the device (shown in Figure 1).

The device has already found wide application in solving a number of biomedical problems: studies on the analysis of variability and reproducibility of LDF and FS channel data in different topographic-anatomical areas of human skin have been carried out [25], the influence of tobacco smoking on the state of the human blood microcirculation system was assessed [26], the possibilities of diagnostics of microcirculatory disorders in men with first diagnosed arterial hypertension are shown [27], extensive studies with patients diagnosed with type 2 DM have established the feasibility of early detection of peripheral circulatory disorders using wearable

devices [28, 29], the possibility of monitoring the efficacy of drug therapy for DM has been demonstrated [30], changes in blood microcirculation in patients who underwent COVID-19 were shown [31], preliminary studies of microgravity influence on the state of astronauts' microcirculatory-tissue systems were carried out [21].

An additional advantage of using wearable devices is the possibility to combine them into a distributed system, which can include up to 8 devices for simultaneous recording of perfusion and fluorescence signals at several points of the body. This approach allows to significantly expand the diagnostic potential of LDF and FS technologies by providing multiple times more diagnostic information.

Figure 2 shows an example of MTS parameters simultaneously registered in different research areas under different external influences with the use of wearable LDF and FS devices. The conducted experiments emphasise the importance of using a distributed system of wearable analysers to record MTS parameters, since the recorded parameters are distinguished by high spatial heterogeneity [32].

Figure 2a shows an example of simultaneous recording of MTS parameters during the occlusion test (OT). Such parameters as index of blood microcirculation and normalised value of fluorescence intensity were evaluated during the measurements. The aim of this experiment was to investigate the effect of occlusion test on simultaneously measured signals of LDF and FS. The study areas were the volar surface of the distal phalanx of the third finger and the dorsal surface of the forearm of the right hand 3 cm above the styloid process. The interest in these areas was caused by the fact that the area of the third finger pad has a large number of arteriolo-venular anastomoses (AVA), whereas the skin in the forearm area contains a small number of AVA, which leads to the predominance of nutritive blood flow in this area. The experimental protocol included recording of the baseline perfusion level for 7 min, occlusion for 3 min, and recording of the parameters' recovery to baseline values for 5 min. During OT, there is a characteristic decrease in I_m values due to cessation of arterial blood inflow, with the I_f (fluorescence intensity at 460 nm, normalised to backscattered radiation fluorescence intensity at 365 nm) value measured in the FS channel increasing in the finger region and decreasing in the forearm region. The results of this study demonstrate a multidirectional response of the fluorescence intensity signal during OT in different study areas. An increase in I_f observed in the finger during occlusion indicates a decrease in metabolic rate, which may be caused by local tissue hypoxia. The obtained results allow us to suggest that recorded data on the state of oxidative metabolism of biological tissues may depend not only on the total blood flow intensity in the study area but also on specific features of oxidative metabolism associated with anatomical features of microvasculature.

Figure 2b shows an example of the application of a distributed system of multimodal wearable LDF and FS analysers in a breath-holding test. The analysers were attached to the same measurement areas as previously described. The study involved recording of LDF and FS signals at rest and during

a 15-s breath holding at inspiratory height. The graph shows a significant drop in perfusion during the test, caused by the activation of a specific reflex reaction leading to an increase in vascular tone. This reaction is manifested in the skin of fingers and is accompanied by a simultaneous increase in the fluorescence signal, which may be associated with a decrease in blood filling of the investigated area, leading to a change in its optical properties. However, in the wrist, the dynamics of I_f are less pronounced, which suggests a lower susceptibility to metabolic conditions leading to short-term respiratory arrest in this area.

Thus, the assessment of the intensity of skin fluorescence in dynamics with functional tests reflects changes in the metabolic processes of biological tissues and is a promising diagnostic criterion. At the same time, the use of a multimodal approach with the simultaneous implementation of FS with other biophotonics methods (first of all LDF-method) allows to obtain comprehensive information about the effectiveness and consistency of oxygen and nutrient delivery processes by the circulatory system and their utilisation by biological tissues, which significantly expands diagnostic capabilities.

3 | Wearable Device Application in Clinical Practice and Space Research

3.1 | Wearable Devices in Clinical Diagnostics

Wearable devices implementing LDF and FS measurement channels can be applied in any fields of medicine associated with the development of disorders of peripheral blood circulation and oxidative metabolism of biological tissues. The possibility to combine them into a distributed system is an undeniable advantage of the technology, allowing to significantly reduce the negative impact of spatial heterogeneity of skin perfusion on the diagnostic results and to increase the diagnostic value of the information received [33, 34]. A schematic example of the biotechnical system for research using wearable LDF and FS devices is shown in Figure 3.

The study protocol may involve the use of up to eight portable devices, which are attached to the subject's body in the areas of greatest diagnostic value before the start of the study by the medical specialist responsible for the measurements. The diagnostic value of the area of measurement may be determined, for example, by the patient's medical history, the presence of concomitant pathologies, the presence of pronounced microcirculatory disorders in one of the limbs, or as a result of preliminary research measurements. After signal registration in accordance with a previously approved protocol, the data received in the process of measurement via wireless protocol into the memory of a personal computer are processed, as a result of which the main biomedical parameters are calculated—index of blood microcirculation (I_m , PU), level of nutritive (Im_{nutr} , PU) and shunt blood flow (Im_{shunt} , PU), amplitudes of endothelial (A_E , PU), neurogenic (A_N , PU), myogenic (A_M , PU), respiratory (A_R , PU) and cardiac (A_C , PU) oscillations, intensity of backscattered fluorescence excitation radiation (A_{365} , AU), fluorescence intensity (A_{460} , AU), normalised to backscattered radiation fluorescence intensity (I_f , AU), oxidative metabolism index (OMI, AU).

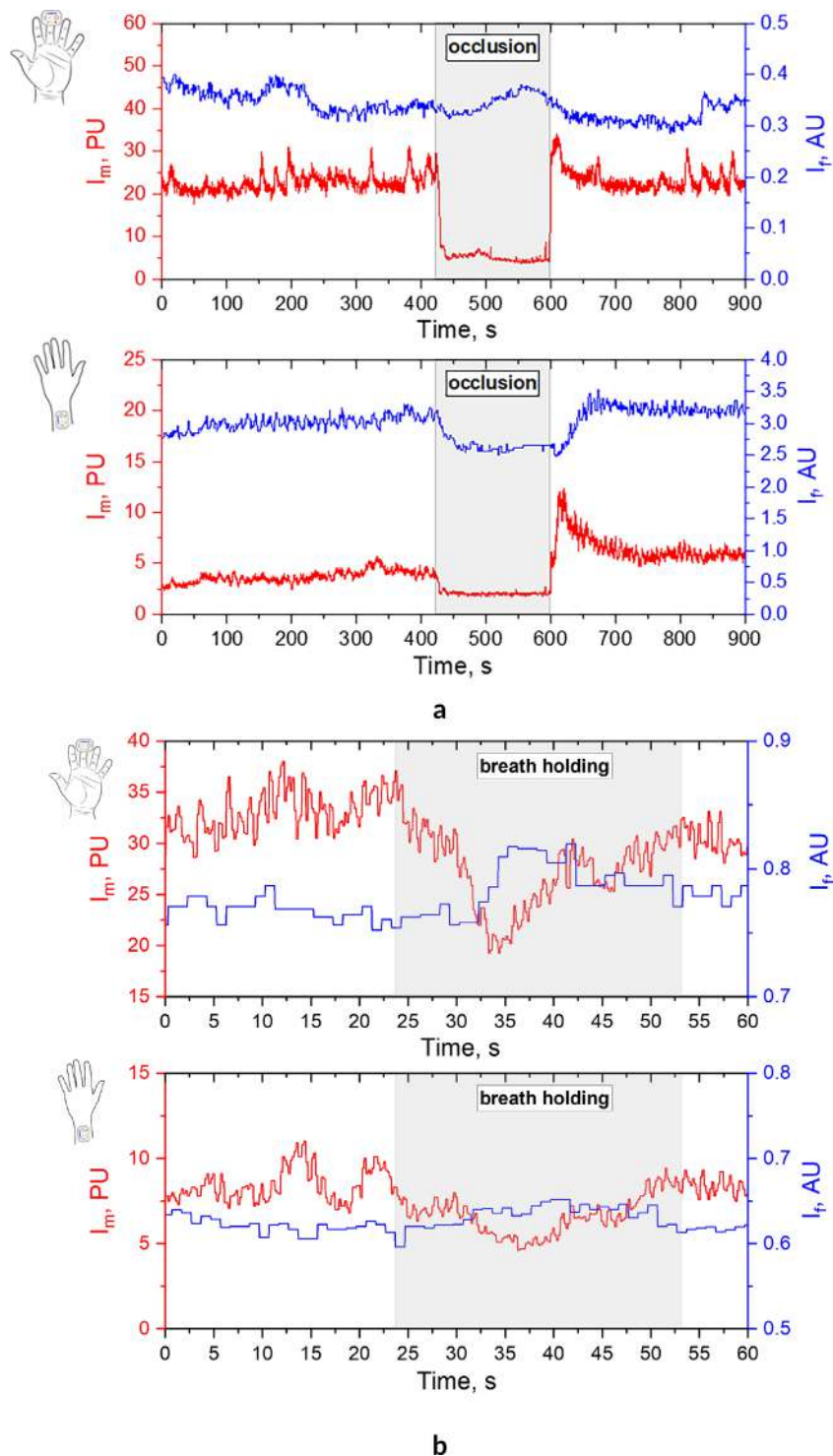


FIGURE 2 | Example of LDF and FS signals recorded by a wearable device for the third finger and forearm during an occlusion test (a) and during breath-holding test (b).

Approaches to calculating these parameters are given in more detail in work [25].

To calculate the values of amplitudes of endothelial, neurogenic, myogenic, respiratory and cardiac oscillations corresponding to the influence of mechanisms of vascular tone regulation, thorax respiratory movements and pulse wave

propagation through vessels, the recorded LDF signal is subjected to wavelet analysis using a continuous Morlet wavelet [29, 35]. Next, using the obtained parameters of the amplitude-frequency spectrum of the LDF signal, it is possible to calculate complex parameters characterising the distribution of microcirculatory blood flow along nutritive and shunt pathways, the total power of the spectrum and the contribution

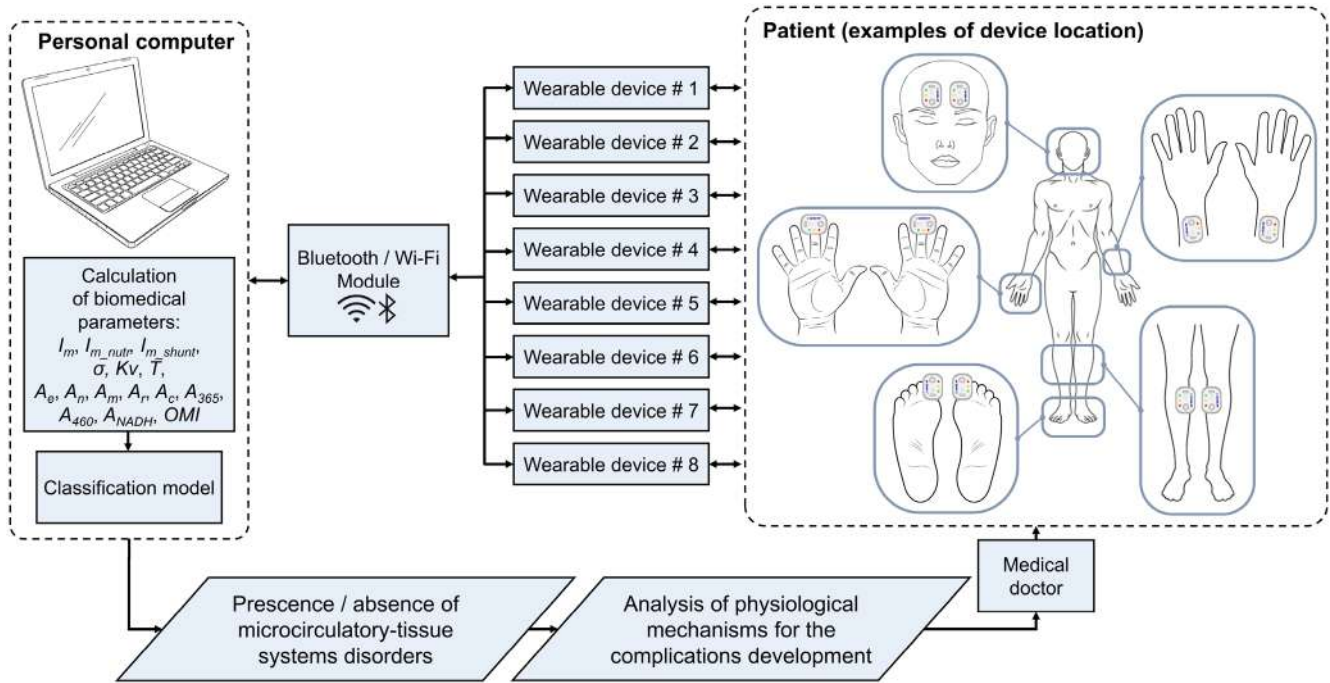


FIGURE 3 | Generalised biotechnical system for biomedical diagnostic research using a distributed system of multimodal wearable analysers in clinical practice.

of individual mechanisms of blood flow regulation to it; on the basis of a multimodal approach, it is possible to calculate the oxidative metabolism index characterising the functioning of the oxygen delivery system and its utilisation by biological tissues [25, 29].

Let us consider the principle of application of the proposed approach to the diagnosis of disorders of microcirculatory-tissue systems on the example of complications caused by the development of type 2 DM. DM is one of the first pathologies in which LDF was used to analyse the maintenance of microcirculatory function [36]. Numerous subsequent studies have confirmed the effectiveness of LDF for assessing changes in cutaneous perfusion in patients with DM in the upper and lower extremities at rest and during the application of functional tests [13], the detection of reduced vasomotion, reduced level of maximal vasodilation during the application of the functional test with acetylcholine and sodium nitroprusside iontophoresis, inadequate microcirculatory response to the application of occlusion test [29].

The FS method is also widely used in the study of metabolic complications of diabetes. It is used to study the accumulation of glycation end products [37], which is a good prognostic marker for the development of diabetic complications [38–41]. The fluorescence of oxidative metabolism coenzymes, NADH and FAD, also contributes greatly to the total skin autofluorescence signal, which can be used to determine the oxidative status of tissues [42, 43].

In our work, carried out with the participation of 26 patients with diagnosed type 2 DM and 31 conditionally healthy volunteers, comparable in age to the main clinical group, it was found in the course of preliminary studies that the regions of

the dorsum of the forearm and the plantar surface of the first toe were characterised by the greatest differences in the studied parameters. It was suggested to use these measurement areas to assess the functional state of the MTS in patients with type 2 DM. Parameters I_m in the forearms and I_{m_nutr} in the toes were found to be the most informative for classifying patients into groups of presence or absence of marked peripheral circulation disorders. It was found that patients with DM are characterised by significantly reduced values of blood microcirculation and the level of nutritive blood flow in the toes, as well as increased values of these parameters in the hands. Decreased perfusion in the toes of patients may result from hyperglycaemia damaging the vessels in the periphery, while increased perfusion in the upper extremities may reflect a compensatory response to peripheral vascular disease in diabetes. Using these parameters, a discriminant function [29] was proposed, which allows to divide patients into groups with presence and absence of peripheral circulation disorders with sensitivity $Se = 0.88$ and specificity $Sp = 0.90$.

Another example of the application of the proposed approach in diagnostics is the study of blood microcirculation disorders in COVID-19 patients. Blood microcirculatory and oxidative metabolic disorders arising in this disease may precede [44] the development of long COVID syndrome, a condition occurring after the initial SARS-CoV-2 and characterised by the appearance of symptoms that continue to negatively affect the patient's life for weeks and months after the initial disease, regardless of viral status [45].

Our study included 50 people who had previously experienced COVID-19 and who reported the presence of symptoms of long COVID syndrome. Patients were divided into two groups according to the severity of symptoms (milder and more severe). The skin of the forehead and the back of the wrists were chosen

as the areas of study of greatest interest. The forehead skin was proposed as the study area due to the fact that the blood supply to this area is via the supraorbital arteries, which are branches of the internal carotid arteries. It can be assumed that the fluctuations of regulation processes and changes in blood circulation registered in the supraorbital artery basin reflect to some extent what is happening in the internal carotid artery basin; a number of modern scientific works are based on this hypothesis [46, 47]. It was also suggested to use the cognitive test as a functional test and to evaluate the relative change in the measured parameters at the stage before and during the cognitive test. The results of the conducted studies showed that patients with more pronounced manifestations of long COVID syndrome are characterised by a greater amplitude of skin autofluorescence in the area of the back of the wrist and a smaller increase in the contribution of cardiac oscillations to the total spectrum power in the scalp area at the stage of cognitive load implementation. Using these parameters, a discriminant function was proposed that allows one to conclude about the presence or absence of pronounced disorders of the functional state of microcirculatory-tissue systems associated with the severe degree of long COVID syndrome with the sensitivity $Se = 0.77$ and specificity $Sp = 0.89$.

3.2 | Wearable Device Application in Space Research

The cardiovascular system is one of the key objects of research in space medicine, since it is subject to significant functional and structural changes both during space flights of various durations and during pre-flight training, which may also lead to the development of early disorders in the absence of proper personalised health control [48]. Pre-flight training includes astronauts' exposure to the simulation of adverse space flight factors. Currently, particular attention is paid to the monitoring of blood circulation parameters at different levels of its organisation both during space missions and ground pre-flight training.

The article [49] reviews the main technologies for monitoring the parameters of the human circulatory system, which have been widely used both in space research and have demonstrated high diagnostic value in clinical practice in cardiology. In particular, the emphasis is placed on the integration of multilevel analysis of hemodynamic characteristics in real time. At the same time, the direction of miniaturisation of medical devices designed for recording hemodynamic parameters is actively developing. There is a trend towards the use of wireless, compact sensors that provide long-term and continuous monitoring, including the assessment of microhemodynamic parameters under various conditions of external influences [50].

In this regard, the adaptation of existing clinical protocols of MTS research for the needs of space medicine, in particular, for the pre-flight training of astronauts, is an urgent task. Figure 4 shows a generalised scheme of the biotechnical system for recording MTS parameters under the influence of simulated space flight factors such as hypoxia, hypobaria, overload, vestibular and orthostatic effects.

The developed protocols include registration of MTS parameters in order to assess the functional response of the system

to certain simulated space flight factors. The biotechnical system presented in Figure 4 can be described as follows: up to four sensors are fixed on the subject, placed in different anatomical areas, the choice of which is conditioned both by the nature of the expected physiological response of the organism to specific external influences and by technical limitations associated with the design features of the simulators used.

Data on the MTS state are recorded at the baseline points of the study—before, during and after the simulator exercise. Signals from sensors are transmitted via wireless transmission channels (Bluetooth/Wi-Fi) to a personal computer, where specialised software calculates diagnostically significant parameters. According to the dynamics of changes in the calculated parameters in the process of exposure to simulated space flight factors, an individual profile of adaptation mechanisms of each subject's organism is built. Based on these data, conclusions are formed about functional reserves of the cardiovascular system, which are then transferred to the doctor for further analysis and planning of individual training programmes for astronauts.

Let us consider in more detail the data recording protocols for each type of simulator used at astronaut's training.

1. Altitude Chamber (Hypoxia and Hypobaria Exposure)

Studies in the altitude chamber are carried out with ascent to altitudes of 5000 and 10000 m. When ascending to a height of 5000 m, the basins of the left and right supraorbital arteries, the dorsum of the left forearm and the palmar surface of the third finger of the left hand are chosen as the areas of study. When ascending to a height of 10000 m, the areas of the supraorbital arteries are replaced by the area of the pectoral muscles on both sides for safety reasons.

MTS parameters are recorded simultaneously at four specified points before the exposure (within 8 min), during ascent, at altitude, during descent and after the exposure is completed. Continuous monitoring makes it possible to record individual reactions of the organism under conditions of hypobaric hypoxia and hypobaria based on the dynamics of changes in peripheral blood flow and oxidative metabolism.

2. Vestibular Impacts

Vestibular examinations are performed on a special vestibular chair in two modes: intermittent and continuous rotations, with cumulative exposure to Coriolis accelerations. The subject rotates on the vestibular chair around the vertical axis at a rate of 0.5 rotations per second. Movement options include shoulder-to-shoulder head tilts (continuous mode) or 45° forward-backward tilts of the head and torso that activate the otolith organs. These stimuli cause a pronounced autonomic response of the body, including redistribution of blood and lymph aimed at maintaining hemodynamic stability. MTS parameters are recorded before and after rotations (8 min each), as well as during and between rotations. The registration areas include the basins of supraorbital arteries, the dorsum of the wrist and the pad of the third finger of the left hand.

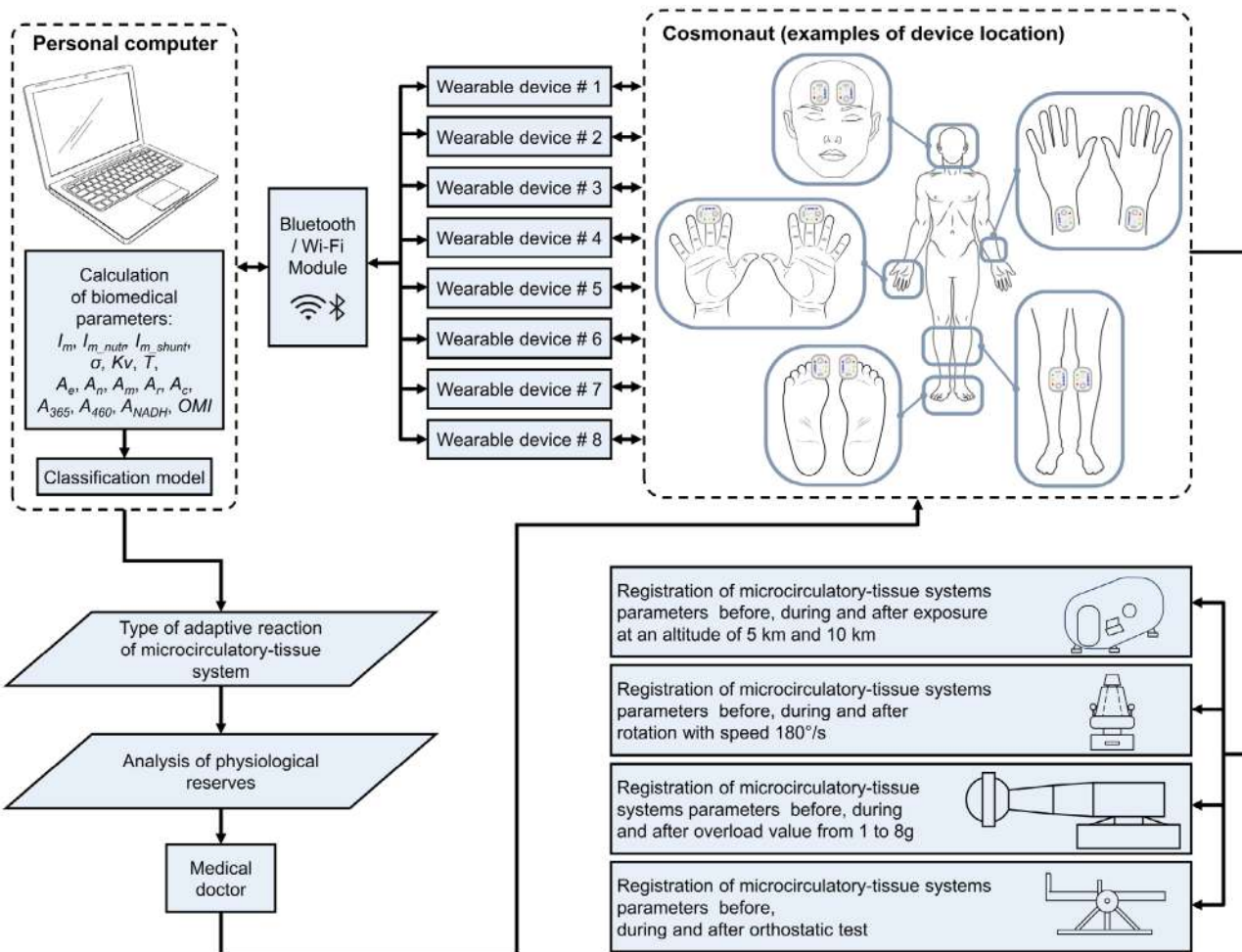


FIGURE 4 | Biotechnical system for biomedical diagnostic research using a distributed system of multimodal wearable analysers when the human body is exposed to certain simulated space flight factors.

3. Centrifuge Rotations (Overloads Exposure)

Overload simulations are performed using 7- and 18-m radius centrifuges. The standard protocol includes two modes. In the first, the overloads vector is directed along the head-pelvis axis, reaching values of 3 and 5 g. The MTS parameters are recorded at symmetrical points on the temporal region of the head (below the hair growth line) and on the inner surface of the upper third of the shins.

In the second mode, the overloads vector is directed along the 'chest-back' axis with exposure of 4 and 8 g. In this case, the areas of the supraorbital arteries and the inner surface of the upper third of the shins are used. Monitoring is performed before the first exposure, between the first and second stage of overload, after the second stage (8 min each), and continuously during the acceleration and deceleration phases of the centrifuge.

4. Orthostatic Effects

An automated electrically driven tilt table is used to simulate orthostatic effects. The subject is placed on the tilt table, and the recording areas include the supraorbital arterial basins and the inner surface of the shins.

The protocol includes the following steps: 8 min in horizontal position (initial state), anti-orthostasis (head down position) with tilt at -15° and -30° (head below the level of the legs)—5 min at each stage, orthostasis (head up position) with tilt 70° (head above the legs) for 20 min, return to horizontal position—8 min. All stages are performed sequentially, without pauses between them.

Testing and validation of the methods for recording MTS parameters under the influence of certain simulated space flight factors was carried out in the Yu.A. Gagarin Research and Test Cosmonaut Training Center (GCTC). The tested subjects were 22 astronauts with and without space flight experience. The experimental studies were carried out during the annual scheduled training of astronauts and did not create additional stress on the organism.

Measurements in the pressure chamber revealed that a decrease in saturation at an altitude of 5000 m is accompanied by activation of the myogenic mechanism in the forehead skin and the neurogenic mechanism in the wrists. This indicates an increase in the number of functioning capillaries and activation of the trophic function of the microvascular bed through activation of the sympathetic nervous system. Also, after the end of the effect of the hypoxic factor on the skin of the basins of the supraorbital arteries, activation of blood flow fluctuations related to the

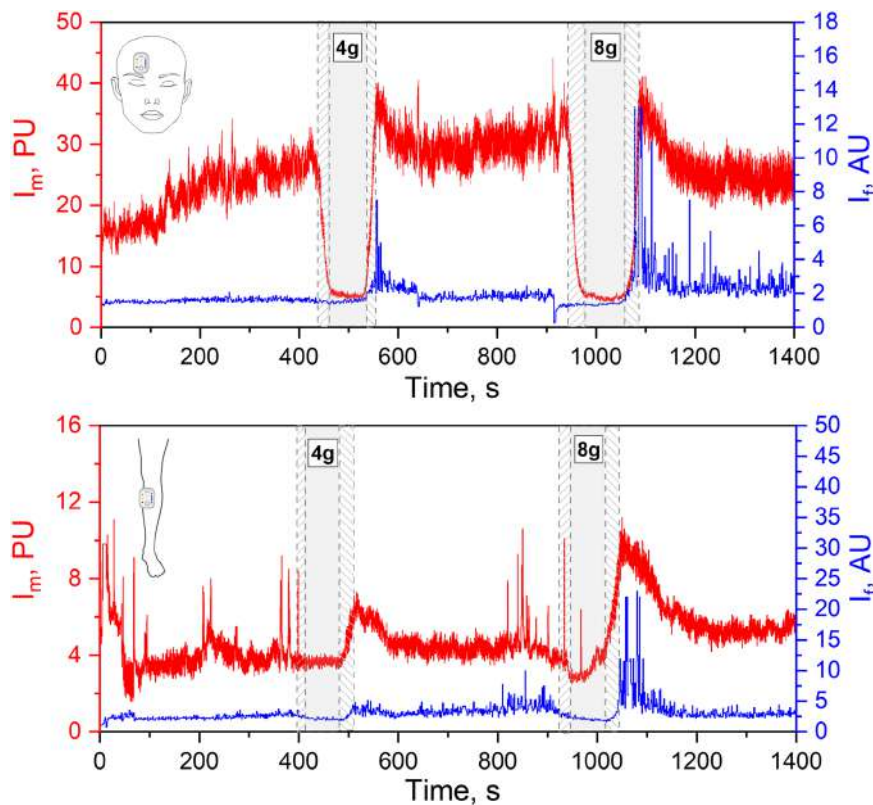


FIGURE 5 | Example of LDF (I_m) and FS (normalised I_f) signals recorded by a wearable device during overload exposure during centrifuge rotations in the forehead and shin regions. The shaded area shows the acceleration and deceleration times of the centrifuge. The grey area is the plateau with fixed overload setting.

cholinergic subrange is observed [51]. However, after the end of hypoxia, the amplitudes of the active mechanisms of blood flow regulation decrease, which indicates vasoconstriction in the peripheral circulation.

Preliminary studies on the centrifuge have shown that overloads in the direction ‘chest-back’ cause a significant decrease in peripheral blood flow in the investigated areas (Figure 5), which is a manifestation of blood centralisation in response to the subject’s compensation of the effect of overload by deep breathing and muscle tension. After the end of the overloads exposure, there is an increase in blood flow in the microcirculatory part of the cardiovascular system, in particular, directly into the nutritive channel, which is the result of the work of local compensatory mechanisms of vascular tone regulation. At the same time in the period of recovery after overloads of 8 g, it is possible to suggest the acceleration of metabolic processes, based on the decrease in the normalised amplitude of fluorescence. The general good tolerance of overloads reflects the correct work of compensation mechanisms of blood redistribution during rotations.

Exposure to 3 and 5 g overloads in the direction of ‘head-pelvis’ is more difficult for the organism. Figure 6 shows representative plots of blood microcirculation index for the temporal areas and shins (a) and microcirculation index and normalised amplitude of fluorescence in the shins (b).

During the centrifuge acceleration phase (shaded area before the start of the overload effect), the first subject (a) shows a decrease in the index of microcirculation in the temporal area and

a simultaneous increase of this parameter in the shin, which corresponds to the expected redistribution of blood flow under the overload’s exposure in the ‘head-pelvis’ direction. Application of the compensation mechanisms in the form of active tension of lower limbs’ skeletal muscles promotes partial restoration of blood flow in the temporal area, which remains at a stable level until the centrifuge stops completely.

However, during the 5 g overload exposure, resistance to blood redistribution in the caudal direction becomes difficult. This is manifested as a further increase in perfusion in the shins and a simultaneous decrease in blood flow in the temporal areas, the level of which is restored only in the phase of centrifuge deceleration. Thus, despite the overall satisfactory load tolerance, this subject shows limited efficiency of compensatory mechanisms of regional blood flow regulation under 5 g overload in the ‘head-pelvis’ direction.

The second subject has the following peculiarities when analysing the parameters of the microcirculatory bed in the shin area. In the phase of both 3 g and 5 g overloads, there is an increase in perfusion in the skin of the shins. This is probably caused by a decrease in vascular tone due to insufficient contraction of lower limb muscles. Nevertheless, adequate tolerance of overload in this case is ensured due to effective breathing technique aimed at stabilisation of intrathoracic pressure and central haemodynamics. Oxidative metabolism in this case shows the properties of a more inert system: its activation (reduction of NADH fluorescence) starts from the moment of the centrifuge rotation beginning and remains

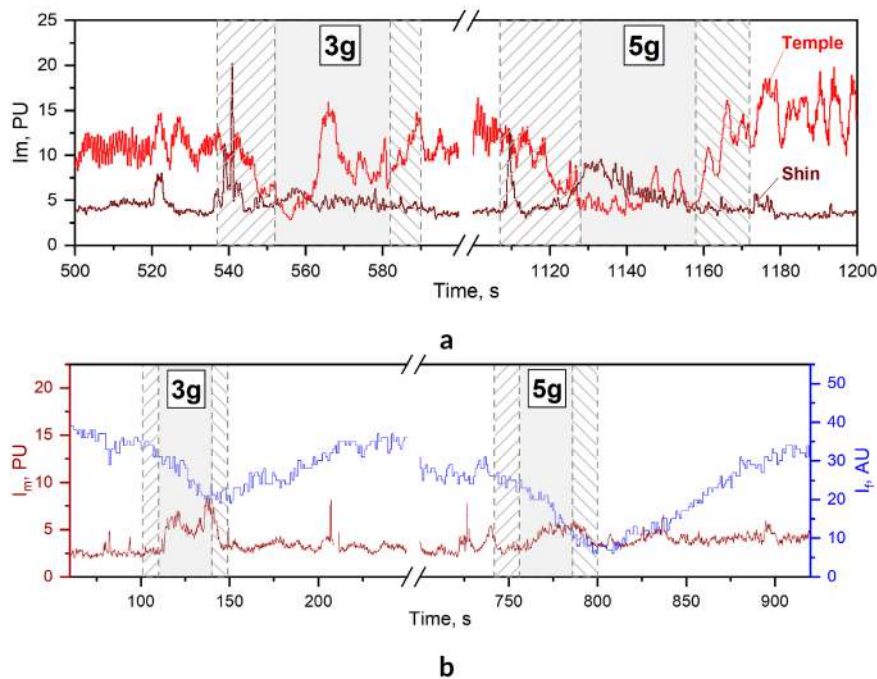


FIGURE 6 | Examples of the index of microcirculation in the temporal areas and shin regions (a) and the index of microcirculation and normalised amplitude of fluorescence in the shin region (b) during 3 and 5 g overload exposure. The shaded area shows the acceleration and deceleration times of the centrifuge. The grey area is the plateau with fixed overload setting.

during the whole period of exposure and recovery to the basic values occurs with a pronounced delay after the overload termination. Thus, a high diagnostic value of data obtained using a distributed system of wearable analysers has been demonstrated. Integration of peripheral blood flow and oxidative metabolism of biotissues allows for an in-depth assessment of the efficiency of adaptation mechanisms to overload and individual compensation strategies.

When performing vestibular impacts, blood redistribution in the microcirculatory bed of the circulatory system also occurs; however, routine registration of microcirculatory-tissue systems parameters has not been performed before due to methodological limitations associated with stationary and fibre-optic design of flowmeters, the complexity of fixing sensors on the volunteer and the impossibility of tracking the influence of motion artefacts on the recorded signal. At present, there are only single publications in the scientific literature showing the high potential of recording microcirculatory flow parameters for predicting motion sickness during Coriolis rotations. For example, the authors Kolev, Möller et al. [52] recorded by means of the LDF method a sharp increase in microcirculatory blood flow in the forehead skin in the first minute after the beginning of rotation with a simultaneous decrease in perfusion in the index finger, which preceded the development of motion sickness and urges to vomit. In the work of another research group [53], nausea occurring during motion sickness during rotations was accompanied by an increase in blood flow in the forearm of volunteers, indicating a decrease in sympathetic activity in this vascular bed. However, there is evidence [54] suggesting that in both groups with good and poor tolerance to vestibular stimulation there is an initial decrease in cutaneous (finger) blood flow, followed by a steady increase and subsequent return to baseline throughout the stimulation, but the increase was greater in the group were

subjects experienced nausea, consistent with a progressive decrease in sympathetic nerve activity.

Thus, in the described works it is shown that poor tolerance to vestibular impacts with the onset of nausea occurs after redistribution of circulating blood volume from the limbs in the cranial direction immediately after the start of Coriolis rotations with the subsequent decrease in sympathetic activity of the skin, manifested in a significant increase in tissue perfusion of the forearm skin. Due to the appearance of a distributed system of portable multimodal MTS analysers, it became possible to study the peculiarities of peripheral blood flow and oxidative metabolism of biotissues of volunteers with good tolerance to vestibular impacts. Thus, the data obtained during vestibular testing of astronauts in GCTC show the following results.

All subjects performed the 10 min vestibular test, but they can be conditionally divided into two groups with good and satisfactory tolerance. Figure 7 shows representative graphs of blood microcirculation index (red) and normalised fluorescence amplitude (blue) of subjects with good (a) and satisfactory (b) tolerance to vestibular impacts.

The first subject is characterised by a gradual increase in the index of blood microcirculation in the forehead skin during the first 3.5 min, more pronounced on the right side, followed by its decrease, most noticeable in the area of the left supraorbital artery basin. The decrease in blood flow in the forehead region is accompanied by an active increase in perfusion in the finger area and an increase in oscillatory activity. In the forearm region, the appearance of low-frequency oscillations is registered amid a stable perfusion level comparable with the baseline values. It is noteworthy that the level of normalised

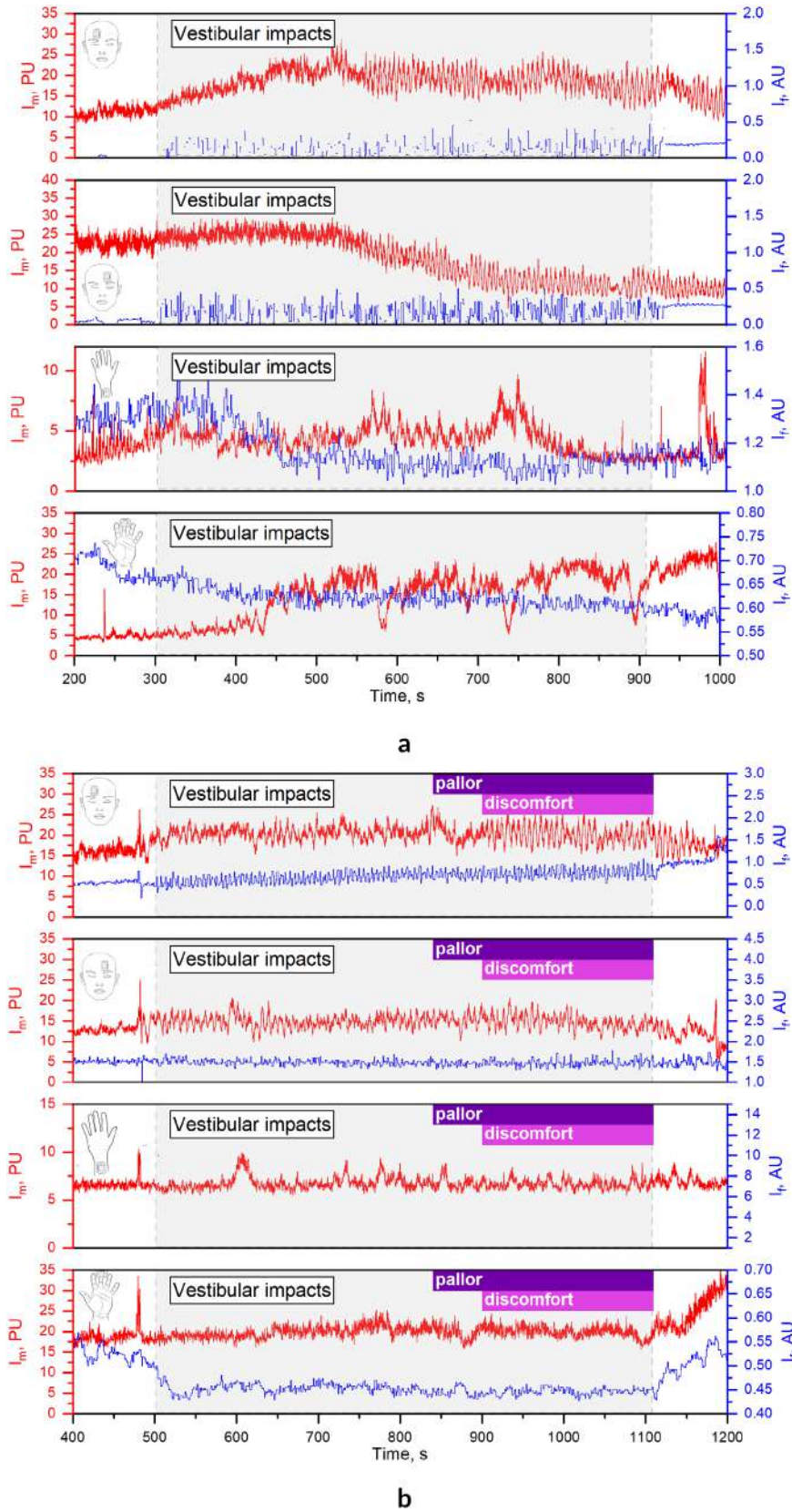


FIGURE 7 | Examples of the index of blood microcirculation and normalised amplitude of fluorescence in case of good (a) and satisfactory (b) tolerance to vestibular impacts.

amplitude of fluorescence in the forehead region remains relatively stable, whereas in the skin of the finger and wrist there is a decrease both during the rotation period and after

its completion. This may indicate an increase in the intensity of oxidative metabolism, which is not caused by changes in circulating blood volume.

Despite the fact that all astronauts endured 10 min of vestibular impacts without pronounced nausea, the appearance of subjective discomfort was noted in some subjects. An example of the MTS data of such a volunteer is presented in Figure 7b.

A characteristic feature is the absence of pronounced perfusion changes throughout the test, which is subsequently accompanied by skin pallor and subjective discomfort. In the skin of the wrist of this subject, already from the first seconds of rotation, a decrease in fluorescence is observed, remaining at a low level until the end of the test, which may indicate the activation of metabolic processes. However, despite the subsequent increase in perfusion, the intensity of metabolism decreases after the end of the test. Thus, on the basis of the obtained data we can conclude that there is no characteristic decrease in sympathetic activity of the skin in case of high tolerance to vestibular impacts. Maintenance of microhomeostasis in such conditions is provided due to coordinated work of tone-forming mechanisms of blood flow and adaptive change in the intensity of oxidative metabolism of cells.

The key factors contributing to high resistance to vestibular impacts are timely initiation of adaptation cascade and severity of changes in microcirculatory parameters. On one hand, it contributes to maintaining the functional state of the organism at an optimal level; on the other hand, it does not lead to excessive deactivation of sympathetic regulation of the cutaneous vascular network. The use of distributed portable multimodal devices allows us to assume the degree of individual tolerance of functional effects already in the first minutes of vestibular effects.

The results of tilt table studies have shown that the body adapts to a new body position due to the activation of both active (mainly neurogenic and myogenic) and passive (cardiac) regulatory mechanisms. When assessing group changes, an increase in the amplitude of pulse wave oscillations is observed in the positions of antiorthostasis both in the shins and the skin of the forehead. In the orthostasis position, on the contrary, myogenic (forehead skin) and neurogenic (shin skin) mechanisms are activated. Thus, the active role of microvascular tone regulation mechanisms in maintaining homeostasis under orthostatic loads is shown.

Registration of microcirculatory-tissue system parameters within the framework of all four protocols allows us to obtain a comprehensive individual picture of the adaptation capabilities of the organism, to assess the functional reserves of the MTS and the circulatory system as a whole. These data are of high value for personalisation of the training process and medical support of astronauts training. The personalised approach is especially relevant in the context of forthcoming long-term space missions, construction of new orbital stations, as well as preparation for manned expeditions to the Moon and Mars.

4 | Conclusion

This paper demonstrates the principle of implementation of wearable multimodal devices implementing diagnostic channels of laser Doppler flowmetry and fluorescence spectroscopy. Compact wireless implementation, absence of optical fibre for

probing biotissues and the possibility of combining several devices into a distributed system for simultaneous investigation of several areas of interest open wide prospects for the application of wearable devices in various fields of medicine and in physiological studies to assess the influence of various factors on the state of microcirculatory-tissue systems. The devices are widely used in various clinical applications, including the diagnosis of MTS abnormalities in the development of complications of diabetes mellitus and in patients who have experienced COVID-19.

The application of wearable LDF and FS devices in space medicine is of great interest—both for recording physiological parameters of astronauts directly in zero gravity conditions and during the training for space flight. The use of wearable devices made it possible for the first time to record LDF and FS signals of astronauts during their space flight on the international space station. Preliminary studies have been conducted to demonstrate the possibility of using wearable devices to record physiological parameters of astronauts in real time during pre-flight training with exposure to overloads, hypoxia and hypobaria, orthostatic and vestibular effects.

Acknowledgements

The work was carried out with the financial support of the Russian Science Foundation (project no. 25-25-00546, <https://rscf.ru/project/25-25-00546/>).

Funding

The work was carried out with the financial support of the Russian Science Foundation (project no. 25-25-00546, <https://rscf.ru/project/25-25-00546/>).

Conflicts of Interest

The authors declare no conflicts of interest.

Data Availability Statement

Data supporting the findings of this study are available from the corresponding author, E.V.Z., upon reasonable request.

References

1. C. Krittanawong, N. K. Singh, R. A. Scheuring, et al., "Human Health During Space Travel: State-Of-The-Art Review," *Cells* 12, no. 1 (2022): 40.
2. Y. Wang, D. Dong, W. Zhou, and J. He, "Flexible Wearable Device Applications for Monitoring Astronaut Health: Current Status and Challenges," *Wearable Electronics* 2 (2025): 77–84.
3. J. L. Griffith, K. Cluff, G. M. Downes, et al., "Wearable Sensing System for NonInvasive Monitoring of Intracranial BioFluid Shifts in Aerospace Applications," *Sensors* 23, no. 2 (2023): 985.
4. D. Rizzoni, C. Agabiti-Rosei, G. E. Boari, M. L. Muiesan, and C. De Ciuceis, "Microcirculation in Hypertension: A Therapeutic Target to Prevent Cardiovascular Disease?," *Journal of Clinical Medicine* 12, no. 15 (2023): 4892.
5. X. Li, D. Yuan, P. Zhang, et al., "A Neuron–Mast Cell Axis Regulates Skin Microcirculation in Diabetes," *Diabetes* 73, no. 10 (2024): 1728–1741.
6. V. V. Tuchin, *Handbook of Optical Biomedical Diagnostics* (SPIE Press, 2002), <https://books.google.ru/books?id=U7cNCRwZqtC>.
7. A. Stefanovska, M. Bracic, and H. D. Kvernmo, "Wavelet Analysis of Oscillations in the Peripheral Blood Circulation Measured by Laser

- Doppler Technique,” *IEEE Transactions on Biomedical Engineering* 46, no. 10 (1999): 1230–1239.
8. R. Martini and A. Bagno, “The Wavelet Analysis for the Assessment of Microvascular Function With the Laser Doppler Fluxmetry Over the Last 20 Years. Looking for Hidden Informations,” *Clinical Hemorheology and Microcirculation* 70, no. 2 (2018): 213–229.
9. L. Kralj and H. Lenasi, “Wavelet Analysis of Laser Doppler Microcirculatory Signals: Current Applications and Limitations,” *Frontiers in Physiology* 13 (2023): 1076445.
10. G. A. Holloway, Jr. and D. W. Watkins, “Laser Doppler Measurement of Cutaneous Blood Flow,” *Journal of Investigative Dermatology* 69, no. 3 (1977): 306–309.
11. I. V. Tikhonova, A. V. Tankanag, I. E. Guseva, and A. A. Grinevich, “Analysis of Interactions Between Cardiovascular Oscillations for Discrimination of Early Vascular Disorders in Arterial Hypertension and Type 2 Diabetes,” *Biomedical Signal Processing and Control* 79 (2023): 104222.
12. E. Zharkikh, V. Dremin, E. Zherebtsov, A. Dunaev, and I. Meglinski, “Biophotonics Methods for Functional Monitoring of Complications of Diabetes Mellitus,” *Journal of Biophotonics* 13, no. 10 (2020): e202000203.
13. D. Fuchs, P. P. Dupon, L. A. Schaap, and R. Draijer, “The Association Between Diabetes and Dermal Microvascular Dysfunction Non-Invasively Assessed by Laser Doppler With Local Thermal Hyperemia: A Systematic Review With Meta-Analysis,” *Cardiovascular Diabetology* 16, no. 1 (2017): 11.
14. M. Rossi, A. Carpi, C. Di Maria, F. Galetta, and G. Santoro, “Spectral Analysis of Laser Doppler Skin Blood Flow Oscillations in Human Essential Arterial Hypertension,” *Microvascular Research* 72, no. 1–2 (2006): 34–41.
15. A. I. Zherebtsova, V. V. Dremin, I. N. Makovik, et al., “Multimodal Optical Diagnostics of the Microhaemodynamics in Upper and Lower Limbs,” *Frontiers in Physiology* 10 (2019): 416.
16. E. Higurashi, R. Sawada, and T. Ito, “An Integrated Laser Blood Flowmeter,” *Journal of Lightwave Technology* 21, no. 3 (2003): 591–595.
17. A. N. Serov, J. Nieland, S. Oosterbaan, et al., “Integrated Optoelectronic Probe Including a Vertical Cavity Surface Emitting Laser for Laser Doppler Perfusion Monitoring,” *IEEE Transactions on Biomedical Engineering* 53, no. 10 (2006): 2067–2074.
18. E. Zherebtsov, S. Sokolovski, V. Sidorov, I. Rafailov, A. Dunaev, and E. Rafailov, “Novel Wearable VCSEL-Based Blood Perfusion Sensor,” in *2018 International Conference Laser Optics (ICLO)* (IEEE, 2018), 564.
19. V. Sidorov, Y. L. Rybakov, V. Gukasov, and G. Evtushenko, “A System of Local Analyzers for Noninvasive Diagnostics of the General State of the Tissue Microcirculation System of Human Skin,” *Biomedical Engineering* 55, no. 6 (2022): 379–382.
20. V. Shcheslavskiy, M. Shirmanova, K. Yashin, A. Rück, M. Skala, and W. Becker, “Fluorescence Lifetime Imaging Techniques—A Review on Principles, Applications and Clinical Relevance,” *Journal of Biophotonics* 18 (2025): e202400450.
21. A. Dunaev, “Wearable Devices for Multimodal Optical Diagnostics of Microcirculatory-Tissue Systems: Application Experience in the Clinic and Space,” *Journal of Biomedical Photonics & Engineering* 9, no. 2 (2023): 020201.
22. I. A. Mizeva, E. V. Potapova, V. V. Dremin, et al., “Optical Probe Pressure Effects on Cutaneous Blood Flow,” *Clinical Hemorheology and Microcirculation* 72, no. 3 (2019): 259–267.
23. A. V. Dunaev, E. A. Zherebtsov, D. A. Rogatkin, N. A. Stewart, S. G. Sokolovski, and E. U. Rafailov, “Substantiation of Medical and Technical Requirements for Noninvasive Spectrophotometric Diagnostic Devices,” *Journal of Biomedical Optics* 18, no. 10 (2013): 107009.
24. E. Zharkikh, V. Dremin, and A. Dunaev, “Sampling Volume Assessment for Wearable Multimodal Optical Diagnostic Device,” *Journal of Biophotonics* 16, no. 9 (2023): e202300139.
25. Y. I. Loktionova, E. Zharkikh, V. Parshakova, V. Sidorov, and A. Dunaev, “Wearable Multimodal Optical Analyzers: Physiological Variability and Reproducibility of Measurements,” *Journal of Biophotonics* 18, no. 4 (2025): e202400527.
26. M. Saha, V. Dremin, I. Rafailov, A. Dunaev, S. Sokolovski, and E. Rafailov, “Wearable Laser Doppler Flowmetry Sensor: A Feasibility Study With Smoker and Non-Smoker Volunteers,” *Biosensors* 10, no. 12 (2020): 201.
27. A. Fedorovich, Y. I. Loktionova, E. Zharkikh, et al., “Skin Microcirculation in Middle-Aged Men With Newly Diagnosed Arterial Hypertension According to Remote Laser Doppler Flowmetry Data,” *Microvascular Research* 144 (2022): 104419.
28. E. A. Zherebtsov, E. V. Zharkikh, Y. I. Loktionova, et al., “Wireless Dynamic Light Scattering Sensors Detect Microvascular Changes Associated With Ageing and Diabetes,” *IEEE Transactions on Biomedical Engineering* 70, no. 11 (2023): 3073–3081.
29. E. Zharkikh, Y. Loktionova, and A. Dunaev, “Microcirculatory Dysfunction in Patients With Diabetes Mellitus Detected by a Distributed System of Wearable Laser Doppler Flowmetry Analysers,” *Journal of Biophotonics* 17, no. 11 (2024): e202400297.
30. E. Zharkikh, Y. I. Loktionova, V. Sidorov, A. Krupatkin, G. Masalygina, and A. Dunaev, “Control of Blood Microcirculation Parameters in Therapy With Alpha-Lipoic Acid in Patients With Diabetes Mellitus,” *Human Physiology* 48, no. 4 (2022): 456–464.
31. E. V. Zharkikh, Y. I. Loktionova, A. A. Fedorovich, A. Y. Gorshkov, and A. V. Dunaev, “Assessment of Blood Microcirculation Changes After COVID-19 Using Wearable Laser Doppler Flowmetry,” *Diagnostics* 13, no. 5 (2023): 920.
32. A. V. Dunaev, V. V. Dremin, E. A. Zherebtsov, et al., “Individual Variability Analysis of Fluorescence Parameters Measured in Skin With Different Levels of Nutritive Blood Flow,” *Medical Engineering & Physics* 37, no. 6 (2015): 574–583.
33. M. Sorelli, Z. Stoyneva, I. Mizeva, and L. Bocchi, “Spatial Heterogeneity in the Time and Frequency Properties of Skin Perfusion,” *Physiological Measurement* 38, no. 5 (2017): 860–876.
34. I. Mizeva, E. Potapova, V. Dremin, I. Kozlov, and A. Dunaev, “Spatial Heterogeneity of Cutaneous Blood Flow Respiratory-Related Oscillations Quantified via Laser Speckle Contrast Imaging,” *PLoS One* 16, no. 5 (2021): e0252296.
35. A. Tankanag and N. Chemeris, “Application of the Adaptive Wavelet Transform for Analysis of Blood Flow Oscillations in the Human Skin,” *Physics in Medicine & Biology* 53, no. 21 (2008): 5967–5976.
36. M. Oimomi, S. Nishimoto, S. Matsumoto, H. Hatanaka, K. Ishikawa, and S. Baba, “Evaluation of Periflux Blood Flow Measurement in Diabetic Patients With Autonomic Neuropathy,” *Diabetes Research and Clinical Practice* 1, no. 2 (1985): 81–85.
37. A. Twarda-Clapa, A. Olczak, A. M. Białkowska, and M. Koziółkiewicz, “Advanced Glycation End-Products (AGEs): Formation, Chemistry, Classification, Receptors, and Diseases Related to AGEs,” *Cells* 11, no. 8 (2022): 1312.
38. E. G. Gerrits, H. L. Lutgers, N. Kleefstra, et al., “Skin Autofluorescence: A Tool to Identify Type 2 Diabetic Patients at Risk for Developing Microvascular Complications,” *Diabetes Care* 31, no. 3 (2008): 517–521.
39. V. R. Aroda, B. N. Conway, S. J. Fernandez, et al., “Cross-Sectional Evaluation of Noninvasively Detected Skin Intrinsic Fluorescence and

Mean Hemoglobin a1c in Type 1 Diabetes,” *Diabetes Technology & Therapeutics* 15, no. 2 (2013): 117–123.

40. E. Sugisawa, J. Miura, Y. Iwamoto, and Y. Uchigata, “Skin Autofluorescence Reflects Integration of Past Long-Term Glycemic Control in Patients With Type 1 Diabetes,” *Diabetes Care* 36, no. 8 (2013): 2339–2345.

41. M. Noordzij, D. Mulder, P. Oomen, et al., “Skin Autofluorescence and Risk of Micro- and Macrovascular Complications in Patients With Type 2 Diabetes Mellitus—A Multi-Centre Study,” *Diabetic Medicine* 29, no. 12 (2012): 1556–1561.

42. V. V. Dremine, E. A. Zherebtsov, V. V. Sidorov, et al., “Multimodal Optical Measurement for Study of Lower Limb Tissue Viability in Patients With Diabetes Mellitus,” *Journal of Biomedical Optics* 22, no. 8 (2017): 085003.

43. D. M. Ciobanu, L. E. Olar, R. Stefan, et al., “Fluorophores Advanced Glycation End Products (AGEs)-to-NADH Ratio Is Predictor for Diabetic Chronic Kidney and Cardiovascular Disease,” *Journal of Diabetes and Its Complications* 29, no. 7 (2015): 893–897.

44. S. Lopez-Leon, T. Wegman-Ostrosky, C. Perelman, et al., “More Than 50 Long-Term Effects of COVID-19: A Systematic Review and Meta-Analysis,” *Scientific Reports* 11, no. 1 (2021): 16144.

45. A. Raveendran, R. Jayadevan, and S. Sashidharan, “Long COVID: An Overview,” *Diabetes and Metabolic Syndrome: Clinical Research and Reviews* 15, no. 3 (2021): 869–875.

46. D. G. Silverman and R. G. Stout, “Distinction Between Atropine-Sensitive Control of Microvascular and Cardiac Oscillatory Activity,” *Microvascular Research* 63, no. 2 (2002): 196–208.

47. F. Bari, V. Tóth-Szúki, F. Domoki, and J. Kálmán, “Flow Motion Pattern Differences in the Forehead and Forearm Skin: Age-Dependent Alterations Are Not Specific for Alzheimer’s Disease,” *Microvascular Research* 70, no. 3 (2005): 121–128.

48. C. Krittanawong, A. Isath, S. Kaplin, et al., “Cardiovascular Disease in Space: A Systematic Review,” *Progress in Cardiovascular Diseases* 81 (2023): 33–41.

49. T. Scalia, L. Bonventre, and M. L. Terranova, “Devices for Cardiovascular Control: When Space and Earth Tackle Common Challenges,” *Acta Astronautica* 198 (2022): 660–668.

50. F. Michard, “Hemodynamic Monitoring in the Era of Digital Health,” *Annals of Intensive Care* 6, no. 1 (2016): 15.

51. V. Perlit, B. Cotuk, M. Lambertz, et al., “Coordination Dynamics of Circulatory and Respiratory Rhythms During Psychomotor Drive Reduction,” *Autonomic Neuroscience* 115, no. 1–2 (2004): 82–93.

52. O. I. Kolev, C. Möller, G. Nilsson, and L. Tibbling, “Responses in Skin Microcirculation to Vestibular Stimulation Before and During Motion Sickness,” *Canadian Journal of Neurological Sciences* 24, no. 1 (1997): 53–57.

53. B. Cheung and K. Hofer, “Coriolis-Induced Cutaneous Blood Flow Increase in the Forearm and Calf,” *Brain Research Bulletin* 54, no. 6 (2001): 609–618.

54. A. Javid, H. Chouhna, B. Varghese, E. Hammam, and V. G. Macefield, “Changes in Skin Blood Flow, Respiration and Blood Pressure in Participants Reporting Motion Sickness During Sinusoidal Galvanic Vestibular Stimulation,” *Experimental Physiology* 104, no. 11 (2019): 1622–1629.